This article was downloaded by: [University of California, San Diego]
On: 07 August 2012, At: 11:57
Publisher: Taylor & Francis
Informa Ltd Registered in England and Wales Registered Number: 1072954 Registered office: Mortimer House, 37-41 Mortimer Street, London W1T 3JH, UK

Molecular Crystals and Liquid Crystals
Publication details, including instructions for authors and subscription information:
http://www.tandfonline.com/loi/gmcl20

Micelles of PAAm-b-PEO-b-PAAm Triblock Copolymers and Their Binding with Prednisolon

Tatyana Zheltonozhskaya [a], Victoria Nedashkovskaya [a], Vitaliy Khutoryanskiy [b], Yuriy Gomza [c], Sergey Fedorchuk [a], Valeriy Klepko [c] & Sofia Partsevskaya [a]

[a] Faculty of Chemistry, Department of Macromolecular Chemistry, Taras Shevchenko National University of Kyiv, Kyiv, Ukraine

[b] Reading School of Pharmacy, University of Reading, Reading RG6 6AD Berkshire, United Kingdom

[c] Institute for Macromolecular Chemistry of the National Academy of Sciences of Ukraine, Kyiv, Ukraine

Version of record first published: 03 Mar 2011

To cite this article: Tatyana Zheltonozhskaya, Victoria Nedashkovskaya, Vitaliy Khutoryanskiy, Yuriy Gomza, Sergey Fedorchuk, Valeriy Klepko & Sofia Partsevskaya (2011): Micelles of PAAm-b-PEO-b-PAAm Triblock Copolymers and Their Binding with Prednisolon, Molecular Crystals and Liquid Crystals, 536:1, 148/[380]-159/[391]

To link to this article: http://dx.doi.org/10.1080/15421406.2011.538595

PLEASE SCROLL DOWN FOR ARTICLE

Full terms and conditions of use: http://www.tandfonline.com/page/terms-and-conditions

This article may be used for research, teaching, and private study purposes. Any substantial or systematic reproduction, redistribution, reselling, loan, sub-licensing, systematic supply, or distribution in any form to anyone is expressly forbidden.

The publisher does not give any warranty express or implied or make any representation that the contents will be complete or accurate or up to date. The accuracy of any instructions, formulae, and drug doses should be independently verified with primary sources. The publisher shall not be liable for any loss, actions, claims, proceedings, demand, or costs or damages whatsoever or howsoever caused arising directly or indirectly in connection with or arising out of the use of this material.

Mol. Cryst. Liq. Cryst., Vol. 536: pp. 148/[380]–159/[391], 2011
Copyright © Taylor & Francis Group, LLC
ISSN: 1542-1406 print/1563-5287 online
DOI: 10.1080/15421406.2011.538595

Downloaded by [University of California, San Diego] at 11:57 07 August 2012

Micelles of PAAm-*b*-PEO-*b*-PAAm Triblock Copolymers and Their Binding with Prednisolon

TATYANA ZHELTONOZHSKAYA,[1] VICTORIA NEDASHKOVSKAYA,[1] VITALIY KHUTORYANSKIY,[2] YURIY GOMZA,[3] SERGEY FEDORCHUK,[1] VALERIY KLEPKO,[3] AND SOFIA PARTSEVSKAYA[1]

[1]Faculty of Chemistry, Department of Macromolecular Chemistry, Taras Shevchenko National University of Kyiv, Kyiv, Ukraine
[2]Reading School of Pharmacy, University of Reading, Reading RG6 6AD Berkshire, United Kingdom
[3]Institute for Macromolecular Chemistry of the National Academy of Sciences of Ukraine, Kyiv, Ukraine

The IntraPC forming asymmetric PAAm-b-PEO-b-PAAm triblock copolymers (TBCs) composed of poly(ethylene oxide) ($M_v = 6 \cdot 10^3$ and $1.4 \cdot 10^4$) and polyacrylamide of a variable chain length form "hairy-type" micelles in water and "flower-like" micelles at the addition of EtOH > 40 vol%. The specific micellization is developed in TBC aqueous/ethanol solutions (EtOH content < 30 vol %) at the PS introduction. It is caused by the binding of PS with TBC micelles due to hydrogen bonds and hydrophobic interactions. The amorphous structure of TBCs and polymorphic crystalline structures of PS are found. The products of the interaction of TBC and PS contain highly ordered crystalline structures of the drug. But it is possible to avoid the drug crystallization at low PS contents.

Keywords Drug; intramolecular polycomplex; micellization; nanocontainer; triblock copolymer

Introduction

Polymer nanocontainers are very promising for a safe transport of different toxic drugs and biopolymers into certain cells of living organisms [1–3]. One of the simplest manners to obtain nanocontainers is the self-assembly of amphiphilic block copolymers with immiscible polymer components in selective solvents [4]. Resulting micellar or vesicular structures are able to solubilize various organic substances, thus playing a role of nanocontainers [5]. But the creation of micelles of block copolymers with chemically complementary polymer components capable to form

Address correspondence to Tatyana Zheltonozhskaya, Faculty of Chemistry, Department of Macromolecular Chemistry, Taras Shevchenko National University of Kyiv, 64, Volodymyrska Str., Kyiv 01033, Ukraine. E-mail: zheltonozhskaya@ukr.net

the intramolecular polycomplexes (IntraPC) [6] may be an alternative way for a nanocontainer making.

In the present work, a series of the IntraPC forming triblock copolymers (TBCs) PAAm-*b*-PEO-*b*-PAAm containing poly(ethylene oxide) of a variable chain length and polyacrylamide is synthesized by the matrix block copolymerization initiated by Ce^{IV} ions [6]. The micellization of these copolymers in aqueous and aqueous/ethanol solutions and their interaction with a synthetic hormone prednisolon (PS) are studied. Ethanol additives were applied to provide a homogeneous introduction of PS, which is water-insoluble, to TBC solutions.

Experimental

PAAm-b-PEO-b-PAAm triblock copolymers with a variable PEO length were synthesized by the matrix free-radical block copolymerization of acrylamide (AAm) from "Reanal" (Hungary) with poly(ethylene glycols) of molecular weights: $M_{v\mathrm{PEG}} = 6 \cdot 10^3$ (PEG1) and $1.4 \cdot 10^4$ (PEG2) from "Merck" (Germany). Ammonium cerium (IV) nitrate from "Aldrich" (USA) was used as an initiator of the block copolymerization and the AAm homopolymerization. The detailed procedure of synthesis and its matrix mechanism were described earlier [7]. The chemical structure of TBCs was confirmed, and their molecular parameters were determined, by using NMR spectroscopy. ^{1}H NMR spectra were recorded on a 400 MHz Mercury-400 spectrometer from "Varian" (USA) in D_2O ($C = 10\,\mathrm{kg \cdot m^{-3}}$) at 20°C. The molecular weight of PAAm, $M_v = 6.3 \cdot 10^5$, was found by viscosimetry. The sample of commercial PS from "Sigma Aldrich" (USA) was used as a model drug in our experiments.

The micelle formation of TBCs in aqueous and aqueous/ethanol solutions was studied with: i) photography, ii) static light scattering (SLS), and iii) spectrophotometry. A modernized instrument FPS-3 (Russia) containing a light-emitting diode WP7113VGC/A ($\lambda = 520$ nm) from "Kingbright", a controller ADC-CPU^{TM} from "Insoftus" (Ukraine), and the computer program "WINRECORDER" was used for SLS studies. All the measurements were carried out with the vertically polarized incident light and the scattering angle $\theta = 90°$. The turbidity of TBC and TBC + PS solutions was determined at $\lambda = 490$ nm, using a photocolorimeter LMF-72 from "LOMO" (Russia).

The existence of bonds between TBC blocks and PS was established with UV and FTIR spectroscopies. UV spectra of PS, PEO, PAAm, and the polymer/PS blends in aqueous/ethanol solutions were recorded, using a UV/VIS spectrometer "Perkin Elmer Lambda 20" (Sweden). FTIR spectra of PS, TBC, and TBC + PS samples were measured by an instrument "Nexus-470 Nicolet" (USA) with a resolution of $4\,\mathrm{cm^{-1}}$. In all the cases, 32 scans of every spectrum were optimal.

The DSC analysis of the (co)polymers, PS, and the products of TBC with PS interaction, which were isolated from the corresponding blends after 24 h by the centrifugation for 15 min at $6 \cdot 10^3$ rot $\cdot$ min^{-1}, was carried out with a differential microcalorimeter DSC-210 and a thermoanalizer 1090 "Du Pont" (USA). The (co)polymers and TBC + PS products were dried in an evacuated case at ~50°C; for 2 days and a vacuum-desiccator for a week. Then 5–10 mg of every sample were placed in open capsules, cooled with liquid nitrogen, and heated with a rate of $16°\mathrm{C \cdot min^{-1}}$. To define the thermodynamic parameters of structural transitions, the instrument was calibrated with indium and zinc. Moreover, a sapphire crystal

Downloaded by [University of California, San Diego] at 11:57 07 August 2012

(m = 61,66 mg) was heated with each polymer sample to recalculate the heat flow curves in the temperature dependences of the specific heat capacity, C_p.

WAXS studies were carried out, by using an X-ray diffractometer DRON-2.0 [8]. The copolymer films, PS, and their blends were cast of aqueous/ethanol solutions on the Teflon surface and dried on air and in an evacuated case. The preparation of TBC + PS products was described above. The samples with a thickness of ~1 mm were used for measurements. The monochromatic Cu-K_α radiation with $\lambda = 0.154$ nm, filtered by Ni, was provided by an IRIS-M7 generator at an operating voltage of 30 kV and a current of 30 mA. The scattered light intensities were measured by a scintillation detector scanning in 0.2° steps over the range of scattering angles, $\theta = 3$–40°. Diffraction curves were reduced to equal intensities of the primary beam and equal scattering volumes by the known technique [8].

Results and Discussion

The chemical building of TBCs and the examples of ^{1}H NMR spectra for polymer components and one of the TBC samples are shown in Figure 1:

The spectrum of PEG (Fig. 1b) contains only a signal of the protons of methylene groups (**α**) with $\delta = 3.68$ ppm, excluding the signal of a H_2O-d_2 solvent with $\delta = 4.80$ ppm, which is not shown in the figures. In the spectrum of PAAm (Fig. 1c), two groups of signals in the intervals of $\delta = 1.4$–1.8 and 2.1–2.4 ppm are displayed. They could be attributed to the protons of methylene (**β**) and methylene (**γ**) groups of acrylamide links. These results are in full accordance with the known literature data. The appearance of the signals **α**, **β**, and **γ** in TBC spectra (Fig. 1d) confirms the existence of PEO and PAAm blocks in the copolymers. Using the integral intensities (A) of the signals **α** and **β** or **α** and **γ** and the known molecular weights of PEO, the average molecular weights of PAAm blocks were calculated by the relations

$$M_{n\cdot PAAm} = \frac{M_{0\cdot PAAm} \cdot M_{PEO} \cdot A_\beta}{M_{0\cdot PEO} \cdot A_\alpha} \quad \text{or} \quad M_{n\cdot PAAm} = \frac{2 \cdot M_{0\cdot PAAm} \cdot M_{PEO} \cdot A_\gamma}{M_{0\cdot PEO} \cdot A_\alpha},$$

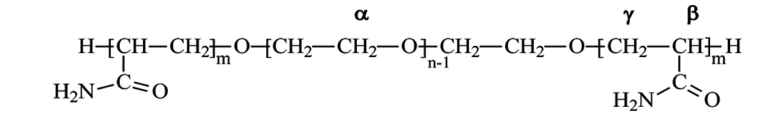

(a)

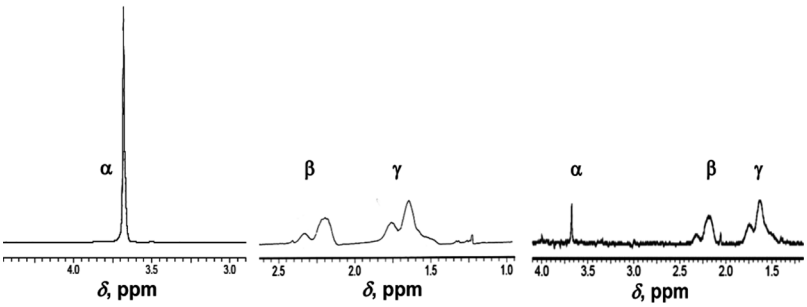

(b) (c) (d)

Figure 1. The examples of ^{1}H NMR spectra in D_2O for: (a) PEG1, (b) PAAm, and (c) TBC1.

Downloaded by [University of California, San Diego] at 11:57 07 August 2012

Downloaded by [University of California, San Diego] at 11:57 07 August 2012

where $M_{0\ \mathrm{PEO}}$ and $M_{0\ \mathrm{PAAm}}$ are the molecular weights of PEO and PAAm units. The values of $M_{\mathrm{nPAAm}} = 1.16 \cdot 10^5$ and $1.045 \cdot 10^6$ were found for TBC1 and TBC2. The total molecular weights of TBC1 and TBC2 calculated as $M_{\mathrm{TBC}} = M_{\mathrm{PEO}} + 2M_{\mathrm{PAAm}}$ are $2.38 \cdot 10^5$ and $2.104 \cdot 10^6$, respectively.

The micellization of amphiphilic block copolymers is widely studied [9]. It is realized in selective solvents due to the insolubility of one of the blocks that initiates a self-assembly of macromolecules in micellar structures with different morphologies [9]. Unlike this, both components of PAAm-b-PEO-b-PAAm triblock copolymers are hydrophilic and are dissolved in water very well. At the same time, they can cooperatively interact with each other by means of hydrogen bonds [6], thus forming hydrophobic parts of the binding of PEO and PAAm segments. That is why the micellization process for such copolymers will be developed in the water medium due to the self-assembly of their hydrophobic bonded parts. Actually, the diluted solutions of TBCs are absolutely transparent, but those with relatively high concentrations demonstrate a weak opalescence (Fig. 2a) which is strengthened with a growth of the PEO length. The onset of micellization can be observed by a significant increase (or a sharp jump) in the scattered light intensity in the copolymer solutions, starting from some critical micellization concentration (*CMC*) [10]. For one of the TBCs, this is shown in Figure 2(a).

Basing on *CMC* values, it is possible to find the Gibbs free micellization energy, using the known relation [6] $\Delta G = RT \cdot \ln CMC$. The results obtained are represented in Table 1:

CMC values decrease, but $-\Delta G^\circ$ numbers increase, when the length of the PEO (and PAAm) block grows. This indicates a rise in the micellar structure stability at the transition from TBC1 to TBC2. With regard for a highly asymmetric character of TBCs (PAAm blocks are essentially longer than the PEO block), the formation of spherical "hairy-type" micelles of TBC macromolecules in a diluted solution (Fig. 2a) can be assumed [6]. A relatively small and friable "core" of these micelles contains H-bonded PEO and PAAm segments, but a large "corona" includes the surplus (not bonded) segments of PAAm. As for an increase in the stability of micellar structures at lengthening the PEO block, it can be explained from the viewpoint of the known fact of increasing the interaction energy between chemically complementary chains with a growth of their lengths [6].

Small ethanol additives (up to ~30 vol. %) enhance noticeably the transparency of TBC solutions, which is accompanied by a significant reduction in the scattered light intensity and keeping its constant value in the studied concentration region (Fig. 2b). Such an effect can be caused by the influence of EtOH on: i) the hydrogen bond system between PEO and PAAm (because of competitive interactions of EtOH with active groups of the blocks) and ii) hydrophobic interactions in a micellar "core" (due to a change of the solvent properties). In any case, small EtOH additives destroy the initial micellar structures of TBCs (a scheme in Fig. 2b). But, at the EtOH content ≥ 40 vol %, the turbidity of TBC solutions begins to grow (Fig. 2c, Fig. 3a). The intense micellization in the range of large EtOH contents takes place due to the insolubility of PAAm chains in ethanol. In fact, large EtOH additives selectively dissolve only PEO blocks. In this case, the values of *CMC* and $-\Delta G^\circ$ (Fig. 2c, Table 1) turn out to be correspondingly less and higher than those for the micellization in aqueous solutions. It is not surprising in view of a very large length of PAAm chains as compared with that of the PEO block. The schematic structure of "flower-like" micelles described for similar TBCs with insoluble side

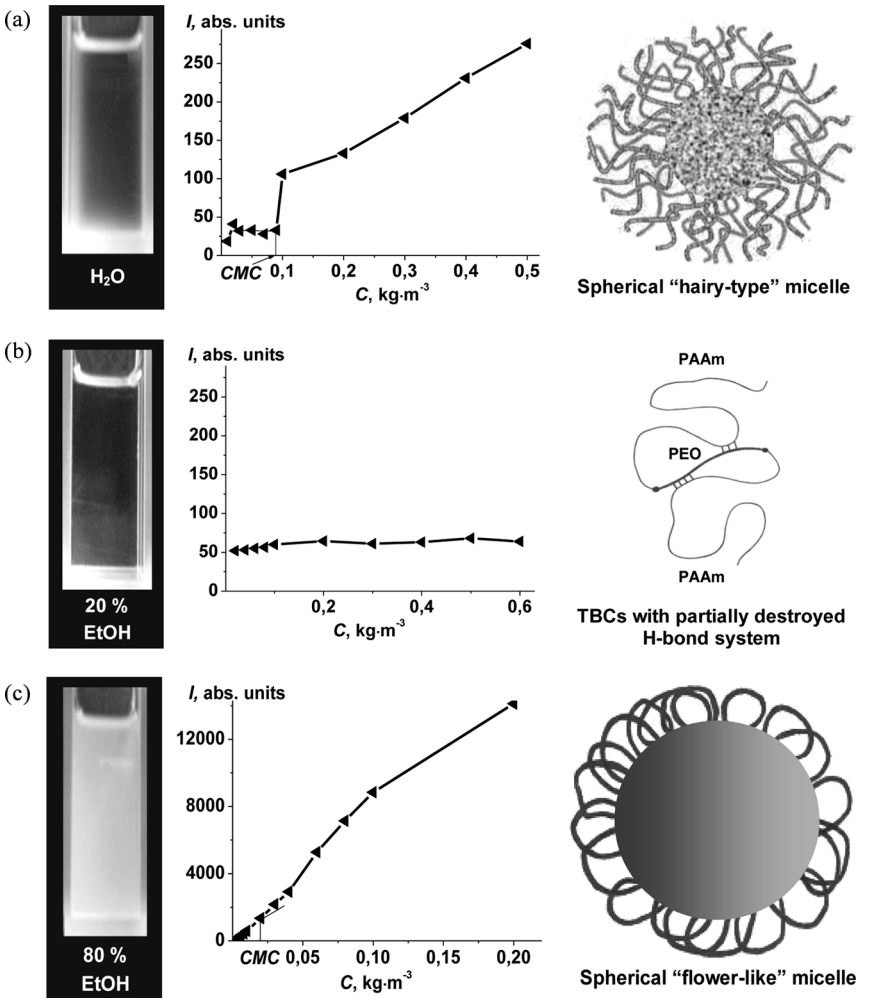

Figure 2. The examples of the TBC1 solution photos together with the concentration changes in the static light scattering intensities and corresponding schemes of TBC molecular/micellar state in: (a) aqueous and (b, c) aqueous/ethanol solutions at (b) 20 and (c) 80 vol % of EtOH ($\lambda = 520$ nm, $\theta = 90°$, a falling light was vertically-polarized).

Table 1. Characteristics of the triblock copolymer micellization in various media

Copolymer	Solvent	CMC[1], $kg \cdot m^{-3}$	$CMC \cdot 10^8$, $mol \cdot dm^{-3}$	$-\Delta G^{\circ}$[2], $kJ \cdot mol^{-1}$
TBC1	H_2O	0.09	37.8	36.15
	$H_2O/EtOH = 30/70$	0.04	8.4	39.82
TBC2	H_2O	0.02	19.0	37.83
	$H_2O/EtOH = 30/70$	0.008	3.8	41.76

[1]The critical micellization concentration.
[2]The Gibbs free micellization energy.

Downloaded by [University of California, San Diego] at 11:57 07 August 2012

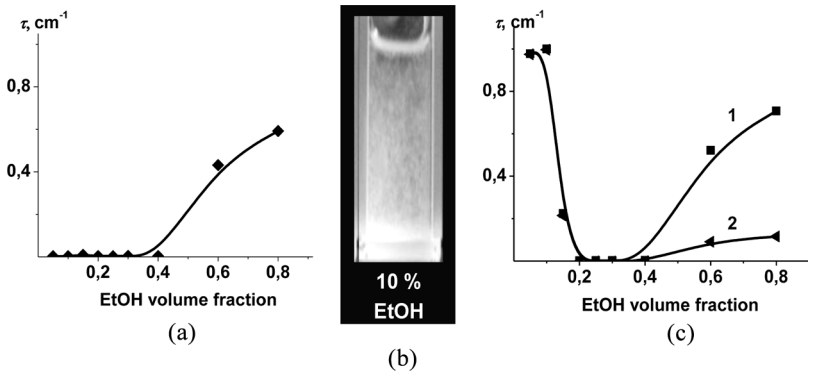

Figure 3. Changes in the turbidity of (a) TBC1 and (c) TBC1 + PS aqueous/ethanol solutions −1 at the EtOH fraction increase, and also (b) a visual representation of the special micellization of TBC macromolecules, initiated by their interaction with PS ($C_{TBC} = 0.4\,kg \cdot m^{-3}$, the composition $\varphi = 0.64\,mol_{PS}/base\text{-}mol_{TBC}$, the contact time $t = 1\,h$, $\lambda = 490\,nm$, $T = 20°C$). The curve 2 (c) represents the difference $\tau_{TBC+PS} - \tau_{TBC}$ in dependence on EtOH content. Analogous picture was observed in TBC2 + PS aqueous/ethanol solutions.

chains [11] is shown in Fig. 2c. Insoluble PAAm blocks form a large "core", but soluble PEO chains are present in the "corona" and ensure the stability for the whole micellar structure.

The addition of PS to TBC solutions at a small EtOH content causes the appearance of special micellar structures similar to large snow-flakes (Fig. 3b and **c**, curve 1). Moreover, the PS introduction intensifies the TBC micellization in the region of high EtOH contents (Fig. 3c, curve 2). These facts testify to the interaction of PS with TBC macromolecules and micelles. Actually, PS molecules include 2 carbonyl and 3 hydroxyl groups (Fig. 4a) which are capable to form H-bonds with different proton-donor and proton-acceptor chemical groups. They contain also 4 hydrophobic cycles and can be involved in hydrophobic interactions with hydrophobic "cores".

UV and FTIR spectroscopy have confirmed the interaction of PS active groups with TBCs. In UV experiments, we studied firstly the EtOH effect on the $n \rightarrow \pi^*$ electronic transition in carbonyl groups of PS (Fig. 4b) and then the binding of these groups with PEO and PAAm separately (Fig. 4c, d). A content of the mixed solvent was $H_2O/EtOH = 70/30$ vol. %, which corresponded to an individual state of TBC macromolecules in aqueous/ethanol solutions (Fig. 2b). An increase in the EtOH content in PS solutions resulted in a characteristic lowering of the wavelength and the intensity of the $n \rightarrow \pi^*$ transition up to its practically full degeneration (Fig. 4b). This indicates the formation of sufficiently strong H-bonds [12] between –OH groups of ethanol and carbonyl groups of PS. PEO does not change the wavelength and the intensity of the mentioned transition (Fig. 4c), but the presence of PAAm diminishes the transition intensity (Fig. 4d, curve 7). Thus, the formation of weak hydrogen bonds between PS carbonyls and $–NH_2$ fragments of PAAm amide groups in the mixed solvent was established.

The participation of −OH groups of PS in the hydrogen bonding with TBC was confirmed with the data of FTIR spectroscopy (they are not shown). The spectrum of commercial crystalline PS (in KBr) demonstrated the following characteristic

Downloaded by [University of California, San Diego] at 11:57 07 August 2012

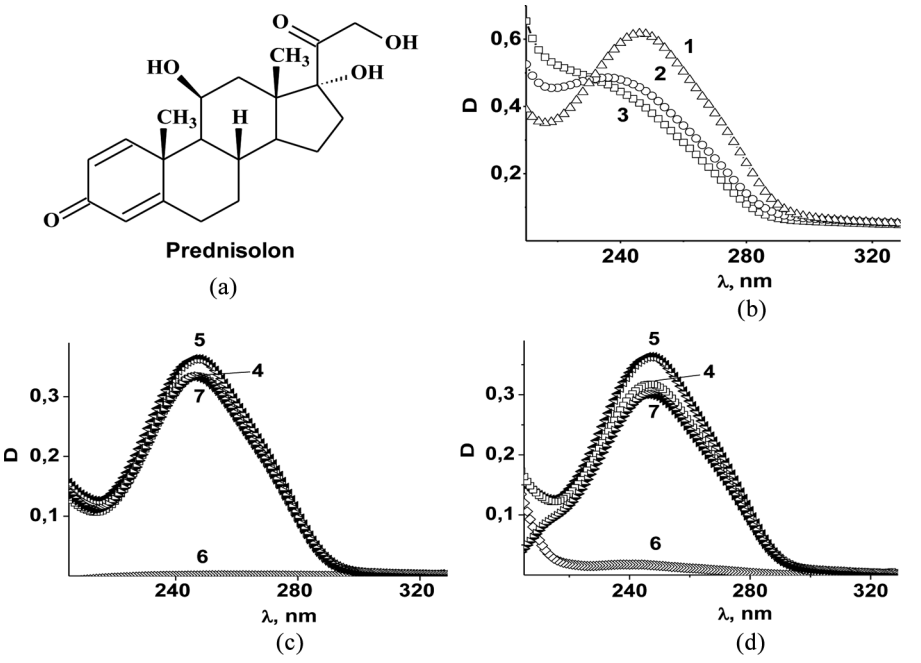

Figure 4. Representation of (a) PS molecular structure as well as UV spectra for: (b) a pure PS in aqueous/ethanol solutions ($C = 1.12 \cdot 10^{-2}\,\mathrm{kg \cdot m^{-3}}$) at 20 −1, 80 −2 and 100 vol % −3 of EtOH, (c) PEG1 + PS and (d) PAAm + PS blends in the mixed ($H_2O/EtOH = 70/30$ vol %) solvent −4, compared to UV spectra of a pure PS ($C = 8.53 \cdot 10^{-3}\,\mathrm{kg \cdot m^{-3}}$) −5 and corresponding polymer ($C_{PEG} = C_{PAAm} = 4 \cdot 10^{-3}\,\mathrm{kg \cdot m^{-3}}$) −6, and also for the differences between UV spectra of the blends and individual polymers −7. $T = 23°C$.

vibration bands: $1707\,\mathrm{cm^{-1}}$ and $1657\,\mathrm{cm^{-1}}$ for free and H-bonded carbonyl groups and also $3575\,\mathrm{cm^{-1}}$, $3464\,\mathrm{cm^{-1}}$, and $3388\,\mathrm{cm^{-1}}$ for H-bonded –OH groups. This means that hydrogen bonds stabilize the crystalline network of PS. The spectrum of a TBC thin film (it was discussed earlier [6] in detail) contains the bands of amide I and amide II at $1662\,\mathrm{cm^{-1}}$ and $1618\,\mathrm{cm^{-1}}$, as well as the bands of $\nu_{N\text{-}H}$ vibrations at $\sim 3470\,\mathrm{cm^{-1}}$, $3345\,\mathrm{cm^{-1}}$, and $3199\,\mathrm{cm^{-1}}$ for H-bonded $-NH_2$ fragments of PAAm amide groups in the structures of *trans*-multimers (two first bands) and *cis-trans*-multimers (the last band). The spectrum of a TBC + PS thin film shows some overlapping bands in the regions of $\nu_{C=O}$, $\nu_{C\text{-}O}$ and $\nu_{C\text{-}O\text{-}C}$ vibrations, which does not allow one to obtain an exact information about the hydrogen bonding between TBC and PS. At the same time, some changes observed in this spectrum in the region of $\nu_{N\text{-}H}$ and $\nu_{O\text{-}H}$ vibrations, namely: i) a decrease in the relative intensity of the band at $3200\,\mathrm{cm^{-1}}$, ii) a high-frequency shift for the band at $3345\,\mathrm{cm^{-1}}$ by $22\,\mathrm{cm^{-1}}$, iii) high-frequency shifts for three above-mentioned PS bands by 9, 32, and $29\,\mathrm{cm^{-1}}$, respectively, and iv) the appearance of an intense $\nu_{O\text{-}H}$ vibration band at $\sim 3290\,\mathrm{cm^{-1}}$, which indicates the participation of –OH groups of PS in the hydrogen bonding with TBC. Basied on these data, we can assume that a specific micellization of TBC macromolecules at small EtOH contents (Fig. 3b) develops because of the hydrogen bonding of drug molecules with both (PEO and PAAm) blocks followed by the hydrophobic segregation of the bound parts. On the other hand, at large

Downloaded by [University of California, San Diego] at 11:57 07 August 2012

Downloaded by [University of California, San Diego] at 11:57 07 August 2012

EtOH contents, PS molecules can concentrate in a "core" of the "flower-like" TBC micelles due to the hydrogen bonding (Fig. 2c) or can stay only at the "core" surface.

The results of DSC studies for PS, PEO, PAAm, TBCs, and the products of the interaction of TBC and PS (obtained in the solvent $H_2O/EtOH = 80/20$ vol. % at the ratio $\varphi = 0.64\,mol_{PS}/base\text{-}mol_{TBC}$ and isolated by a centrifugation) are collected in Figure 5 and in Table 2. The DSC thermogram of commercial PS contains only the endothermic peak at 236.5°C which corresponds to the melting transition (Fig. 5a). Unlike this, a PS sample prepared of a mixed solvent demonstrates two endothermic peaks in the 1st scan of the DSC thermogram (Fig. 5b). The first peak can be attributed to the process of water evaporation from PS monohydrate (PS_{hydr}) [13] which is always formed at the drug crystallization of aqueous solutions. Parameters of the process for PS_{hydr} (and isolated products of the PS binding with

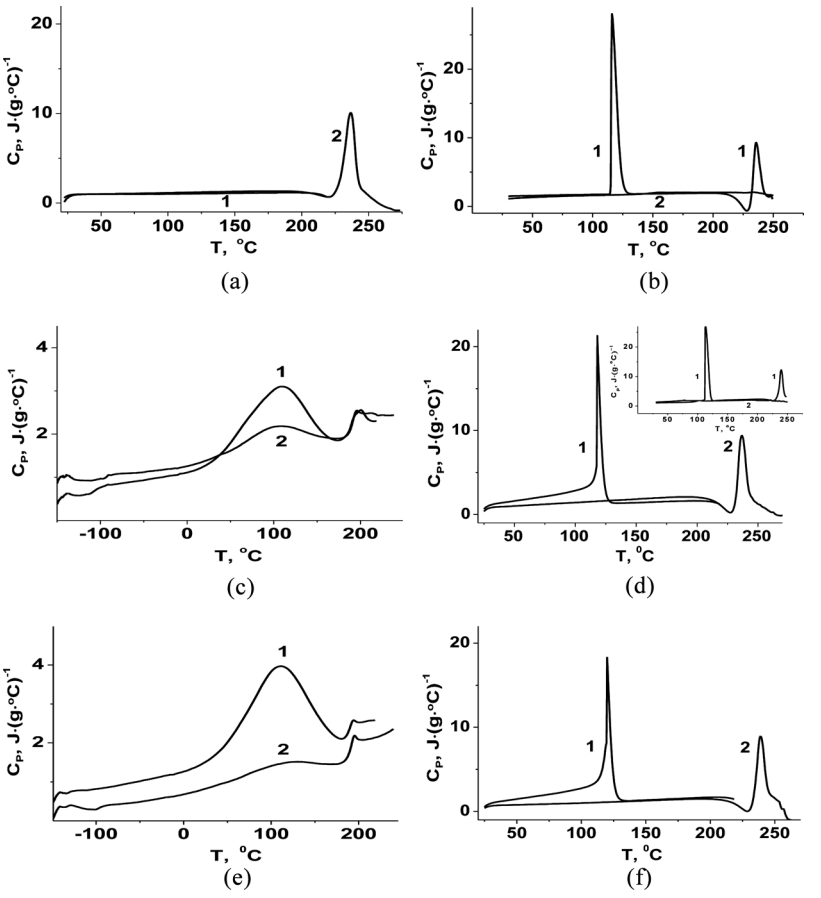

Figure 5. Dependences of the specific capacity *vs* the temperature (the 1-st −1 and 2-nd −2 scans) for: (a) commercial PS, (b) PS monohydrate, dried of its aqueous/ethanol (80/20 vol %) solution, (c) TBC1, (e) TBC2 and also (d,f) products of an interaction of (d) TBC1 and (f) TBC2 with PS ($\varphi = 0.64\,mol_{PS}/base\text{-}mol_{TBC}$), which were isolated of the same mixed solvent. The heating rate was 16 degree $\cdot$ min^{-1}. Figure (d) demonstrates the effect of a scanning regime on DSC thermogram of one of the products.

Table 2. Thermal transition parameters for individual polymer components, the triblock copolymers, prednisolon, and the isolated products of TBC with PS interaction

Substance	Scan	T_g[1], °C	ΔT_g[2], °C	ΔC_p[3], $J \cdot (g \cdot °C)^{-1}$	T_m[4], °C	ΔT_m[2], °C	ΔH_m[5], $J \cdot g^{-1}$	X_c[6], %
PAAm	2	190.9	8.0	0.55	–	–	–	–
PEG1	1	–	–	–	68.6	38	185.6	94.3
	2	–	–	–	64.8	47	154.7	78.6
PEG2	1	–	–	–	68.0	40	186.2	94.6
	2	–	–	–	64.8	49	134.5	68.3
TBC1	2	189.6	8.8	0.65	–	–	–	–
TBC2	2	190.3	9.2	0.75	–	–	–	–
PS	2	–	–	–	236.5	37	101.9	–
PS_{hydr}	1	–	–	–	116.0*	14*	98.4*	–
					236.0	35	84.9	–
TBC1 + PS[7]	1	–	–	–	118.5*	20*	82.0*	–
	2	–	–	–	237.0	37	96.8	–
TBC2 + PS[7]	1	–	–	–	120.0*	22*	72.4*	–
	2	–	–	–	239.0	38	96.2	–

[1]The glass transition temperature.
[2]The temperature range for corresponding thermal transition.
[3]The specific capacity jump.
[4]The melting tenperature.
[5]The melting enthalpy.
[6]The crystallinity degree: $X_{cPEG} = \Delta H_m / \Delta H_m^\circ$, where ΔH_m° is the melting enthalpy for 100% crystalline polymer ($196.8\,J \cdot g^{-1}$).
[7]The compositions of the initial TBC + PS blends $\varphi = 0.64\,mol_{PS}/base\text{-}mol_{TBC}$.

TBCs) are designated in Table 2 by stars. It is seen that, after the PS_{hydr} destruction, the crystallization process exactly before the melting transition takes place (Fig. 5b).

The amorphous homogeneous structure of TBCs is displayed in DSC thermograms by only the glass transition (Fig. 5c,e), whose temperature turns out to be somewhat less than T_g for PAAm (Table 2). Thus, macromolecules of PEG1 and PEG2, having a high crystallinity degree in a bulk state (Table 2), loss completely their crystalline properties in the triblock copolymers. The reasons for this phenomenon were considered earlier [7]. The DSC thermograms of both products of the TBC1 and TBC2 interactions with the drug are shown in Figure 5(d, f). They are fully analogous to the thermogram of PS_{hydr} (Fig. 5b), excluding the facts of some increase in T_m and ΔH_m values (Table 2). It is worth noting also the absence of glass transitions for the copolymer components of both the products. In principle, the last effect is not surprising with regard for a relatively high content of crystalline PS in the initial TBC + PS blends: $w_{PS} = 76.7$ wt.% for TBC1 and 76.4 wt.% for TBC2. As to two first facts, they could be attributed to the formation of more perfect PS microcrystals inside TBC micellar structures during their isolation and drying. It is interesting to consider, in this connection, the wide-angle X-ray scattering (WAXS) data which are represented in Figure 6.

Downloaded by [University of California, San Diego] at 11:57 07 August 2012

Downloaded by [University of California, San Diego] at 11:57 07 August 2012

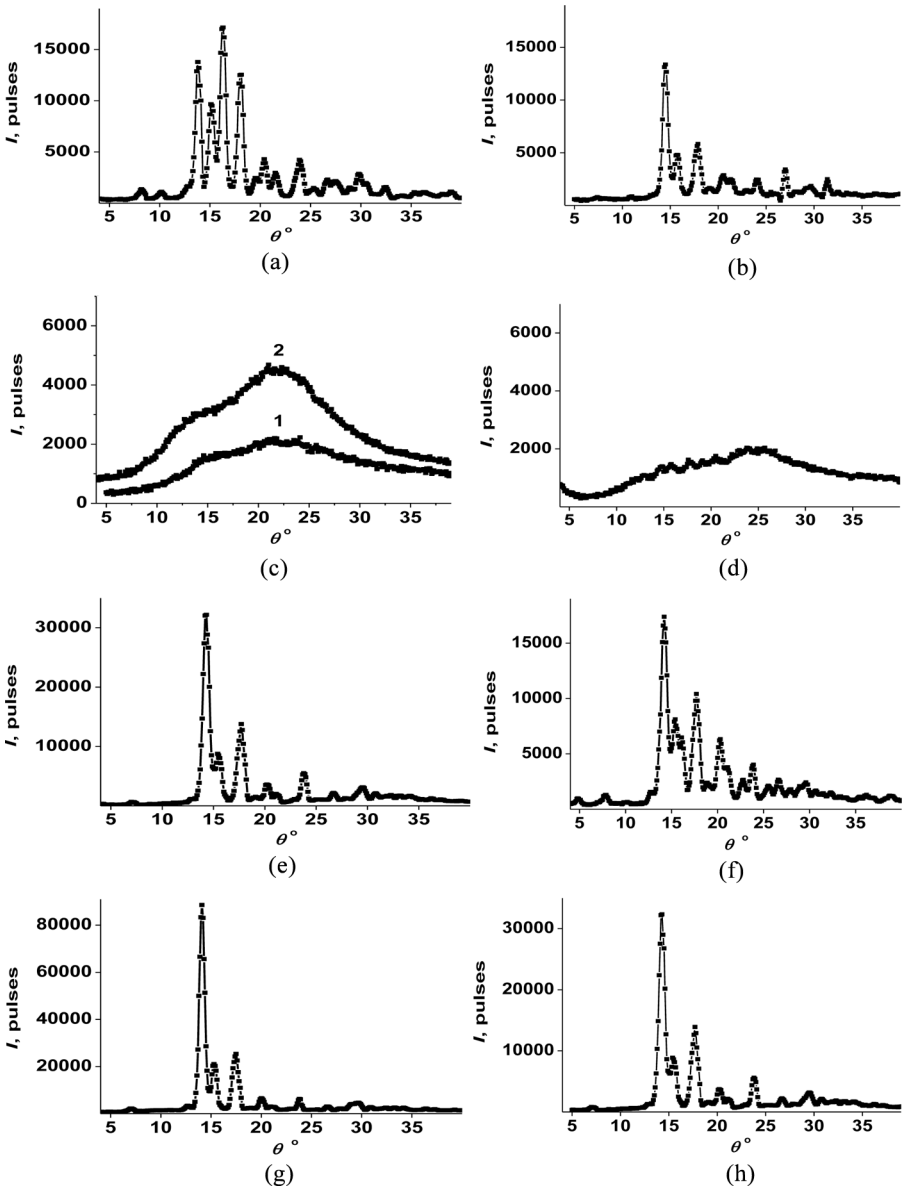

Figure 6. Difractograms (WAXS profiles) for: (a) initial PS and (b) its monohydrate, (c) TBC1 −1 and TBC2 −2, (**d,e**) the blends TBC1 + PS with compositions (d) $\varphi = 0.021$ and (e) $\varphi = 0.42\,\text{mol}_{PS}/\text{base-mol}_{TBC}$, (g) the blend TBC2 + PS with $\varphi = 0.42\,\text{mol}_{PS}/\text{base-mol}_{TBC}$, and also (**f,h**) the products of (f) TBC1 or (h) TBC2 interaction with PS, which were isolated of their blends with $\varphi = 0.42$.

It is seen that the crystalline structures of commercial PS and its monohydrate are polymorphic and essentially differ from each other (Fig. 6a, b, Table 3). Such a result is in full accordance with the data in [13]. The amorphous structure of TBCs is displayed in WAXS profiles by two wide "halos" which are strongly overlapped (Fig. 6c). This is related to the presence of two systems of planes of a paracrystalline

Table 3. Diffraction peak positions in WAXS profiles and the calculated interplane distances for PS and its compositions with the triblock copolymers

				TBC1 + PS ($\varphi = 0.42$)				TBC2 + PS ($\varphi = 0.42$)			
PS		PS_{hydr}		Initial blend		Isolated product		Initial blend		Isolated product	
θ^1, °	d^2, nm	θ, °	d, nm	θ, °	d, nm	θ, °	d, nm	θ, °	d, nm	θ, °	d, nm
13.8	0.641	14.2	0.623	14.3	0.619	14.2	0.623	14.1	0.627	14.3	0.619
15.1	0.586	15.4	0.575	15.4	0.575	15.4	0.575	15.3	0.578	15.4	0.575
16.3	0.543	–	–	–	–	16.1	0.550	–	–	–	–
18.1	0.490	17.6	0.503	17.7	0.500	17.7	0.500	17.5	0.506	17.7	0.500
19.6	0.452	20.3	0.437	20.2	0.439	20.3	0.437	20.0	0.443	20.2	0.439
20.4	0.435	20.9	0.425	21.1	0.421	21.1	0.421	20.9	0.425	21.1	0.421
21.5	0.413	–	–	–	–	22.8	0.390	–	–	–	–
23.9	0.372	23.6	0.377	23.8	0.373	23.9	0.372	23.0	0.386	23.8	0.373

[1]The scattering angle corresponding to the diffraction peak maximum.
[2]The average interplane distance.

lattice in amorphous (co)polymers [7]. The type of a crystalline lattice of PS in two dried TBC + PS blends at $\varphi = 0.42$ (Fig. 6e, g) and one of the isolated products (TBC2 + PS) (Fig. 6h) correspond to that in PS_{hydr} (Table 3). But the leading contribution of the first crystalline peak (at $\theta \approx 14.2°$) to the total scattering picture increases in the compositions. Therefore, a perfection of this crystalline lattice grew. The crystalline lattice of another type as compared with that of PS_{hydr} is formed due to the interaction of TBC1 with PS at the initial content of the blend $\varphi = 0.42$ (Fig. 6f, Table 3). At the same time, the most interesting phenomenon consists in the fully amorphous character of the blend TBC1 + PS at $\varphi = 0.021$ (Fig. 6d, Table 3). The last two results which are obviously related to the more strong interaction of PS with TBC1 micelles as compared with that for TBC2 at $\varphi = 0.42$ (Fig. 6f, Table 3) open a real way for the influence of micellar structures on crystalline properties of different drugs. This problem is very actual and widely discussed in the literature [14].

References

[1] Cameron, N. S., Eisenberg, A., & Brown, R. G. (2002). *Biomacromolecules*, *3*, 124.
[2] Croy, S. R., & Kwon, G. S. (2004). *J. Control. Release*, *95*, 161.
[3] Savić, R., Luo, L., Eisenberg, A., & Maysinger, D. (2003). *Science*, *300*, 615.
[4] Terreau, O., Bartels, C., & Eisenberg, A. (2004). *Langmuir*, *20*, 637.
[5] Choucair, A., Lavigueur, C., & Eisenberg, A. (2004). *Langmuir*, *20*, 3894.
[6] Zheltonozhskaya, T., Permyakova, N., *et al*. (2008). In: *Hydrogen-Bonded Interpolymer Complexes. Formation, Structure and Applications*, Khutoryanskiy, V. V. & Staikos, G. (Eds.), World Scientific: Singapore, Ch. 5, p. 85.
[7] Fedorchuk, S. V., Zheltonozhskaya, T. B., Permyakova, N. M., Gomza, Y. P., Nessin, S. D., & Klepko, V. V. (2008). *Molecular Cryst. Liquid Cryst.*, *497*, 268.
[8] Lipatov, Yu. S., Shilov, V. V., Gomza, U. P., & Kruglyak, N. E. (1982). *X-Ray Methods of Studies of Polymeric Systems*, Naukova Dumka: Kyiv, (in Russian).
[9] Riess, G. (2003). *Prog. Polym. Sci.*, *28*, 1107.

Downloaded by [University of California, San Diego] at 11:57 07 August 2012

[10] Khougaz, K., Astafieva, I., & Eisenberg, A. (1995). *Macromolecules*, *28*, 7135.
[11] Yang, Y., Hua, C., & Dong, C.-M. (2009). *Biomacromolecules*, *10*, 2310.
[12] Pretsch, E., Bullman, P., & Affolter, C. (2000). *Structure Determination of Organic Compounds*, Springer: Berlin.
[13] Li, X.-S., Wang, J.-X., Shen, Z.-G., Zhang, P.-Y., Chen, J.-F., & Yun, J. (2007). *Int. J. Pharm.*, *342*, 26.
[14] Rawlinson, C. F., Williams, A. C., Timmins, P., & Grimsey, I. (2007). *Int. J. Pharm.*, *336*, 42.

Downloaded by [University of California, San Diego] at 11:57 07 August 2012